Simulation on Discharge Inception Voltage Improvement of GIS Spacer with Permittivity Graded Materials (ε-FGM) Using Flexible Mixture Casting Method

Naoki Hayakawa, Yoshitaka Miyaji and **Hiroki Kojima**
Department of Electrical Engineering, Nagoya University
Furo-cho, Chikusa-ku, Nagoya 464-8603, Japan

and **Katsumi Kato**
Department of Electrical Engineering and Information Science,
National Institute of Technology, Niihama College
7-1 Yaguma-cho, Niihama, Ehime 792-0392, Japan

ABSTRACT

For electric field grading in GIS spacers, the application of functionally graded materials (FGM) with spatial distribution of dielectric permittivity (ε) can be one effective solution. In this paper, we propose the flexible mixture casting (FMC) method as a novel and practical technique to fabricate ε-FGM for GIS spacers. We verified that the relative permittivity (ε_r) can be controlled from $\varepsilon_r = 4$ to $\varepsilon_r = 30$ by varying the loading ratio of high permittivity filler particles under the FMC method. Toward the practical application of ε-FGM, we verified the relaxation effect of maximum electric field strength and the improvement effect of discharge inception voltage in SF_6 gas in a simplified GIS spacer model using ε-FGM under the FMC method. Simulation results revealed that the maximum electric field strength can be effectively reduced and the discharge inception voltage can be significantly improved compared with using a constant and uniform permittivity.

Index Terms — **electric field grading, gas insulated switchgear (GIS), spacer, functionally graded material (FGM), permittivity, breakdown voltage**

1 INTRODUCTION

GAS insulated power apparatus, e.g. gas insulated switchgears (GIS) and transmission lines (GIL), are expected to have compact size and reliable electrical insulation performance. The electrical, mechanical and thermal design of gas insulated power apparatus depend on the solid materials of spacers and their composite system with SF_6 gas. Especially, in the electrical insulation design of gas/solid composite systems, the electric field distribution both in the gas space and on the solid insulator surface is crucial due to the highly sensitive nature of SF_6 gas with electric field strength. Thus, electric field control or grading is indispensable for gas insulated power apparatus.

The electric field grading of GIS and GIL has been conducted by shape control of spacers and electrodes, additional or embedded electrodes, etc. However, such conventional techniques have increased structural complexity and the cost of design and manufacturing. Recently, as innovative techniques for electric field grading, non-linear materials [1-3] and functionally graded materials (FGM) [4-6] have been investigated. We have been investigating the application of FGM with spatial distribution of dielectric permittivity (ε) and electrical conductivity (σ) to the spacers of gas insulated power apparatus. So far, we have estimated the relaxation effect of maximum electric field strength in a GIS spacer with ε-FGM and/or σ-FGM, compared with that with a constant value of ε and zero conductivity. We also have fabricated a small sample of ε-FGM with a localized filler distribution in epoxy resin by the centrifugal method to fundamentally verify the concept of FGM [6]. However, the centrifugal method has some possible drawbacks, e.g. difficulty using larger sizes for actual GIS spacers, and reduced mechanical and/or thermal properties due to the localized filler distribution.

From the above background, toward the practical application of an ε-FGM to gas insulated power apparatus, this

---

Manuscript received on 2 December 2017, in final form 8 February 2018, accepted 12 February 2018. Corresponding author: N. Hayakawa..

paper proposes a novel fabrication technique of an ε-FGM, referred to as the flexible mixture casting (FMC) method, in order to overcome the possible drawbacks of the centrifugal method. We evaluated not only the relaxation effect of the maximum electric field strength in a simplified GIS spacer model with ε-FGM using the FMC method, but also its improvement effect of theoretical discharge inception voltage (TDIV), based on the volume-time theory.

2 ε-FGM CONCEPT AND FABRICATION METHOD

2.1 ε-FGM CONCEPT

Suppose a coaxial cylinder of infinite length, with the electrical insulation layer between the inner high voltage electrode and outer grounded electrode is filled with a solid insulator. In general, the permittivity of the solid insulator is constant and uniform. The electric field distribution in the stressed insulation layer has its maximum value at the inner electrode surface and decreases with the increase in distance from the center axis. Here, if the permittivity of the solid insulator is not uniform and has a radial distribution inversely proportional to the distance from the center axis, the electric field strength in the insulation layer is the same or uniform throughout the solid insulator [7]. This is the fundamental concept of ε-FGM with spatial distribution of permittivity.

In the case of GIS spacers with a gas/solid composite insulation system, the electric field distribution in the gas space and on the spacer surface is distorted by the spacer shape and the permittivity difference between the gas and solid insulator. Thus, if the permittivity distribution of the spacer can be arbitrarily controlled by ε-FGM, electric field grading can be realized and optimized, which will contribute to reduced size, simpler configuration, improved breakdown voltage and lower cost of GIS spacers.

2.2 FLEXIBLE MIXTURE CASTING (FMC) METHOD

The availability of ε-FGM for electric field grading has been principally verified by the centrifugal method in our previous work [6]. In the centrifugal method, the radial distribution of permittivity is formed in the centrifugal direction, as shown in Figure 1a, under a centrifugal force several thousand times that of gravity, e.g. 2900-4000 G [6]. Such high centrifugal force is hard to be applied in manufacturing the actual GIS spacers with a large diameter at the transmission voltage level. Also, the centrifugal method forms a localized density distribution of filler particles corresponding to the permittivity distribution. Such localized density distribution of filler particles could reduce the mechanical and/or thermal properties, e.g. withstand stress, lifetime, etc. Therefore, we propose the flexible mixture casting (FMC) method as a novel fabrication method for ε-FGM. Using the FMC method, a longitudinal distribution of permittivity is formed, as shown in Figure 1b, and the density distribution of filler particles can be controlled by varying their loading ratio.

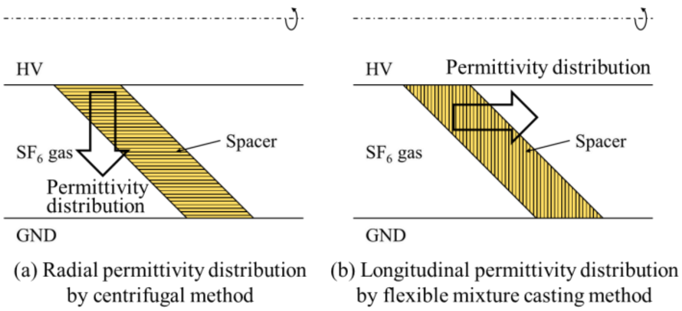

(a) Radial permittivity distribution by centrifugal method (b) Longitudinal permittivity distribution by flexible mixture casting method

Figure 1. Permittivity distribution of ε-FGM.

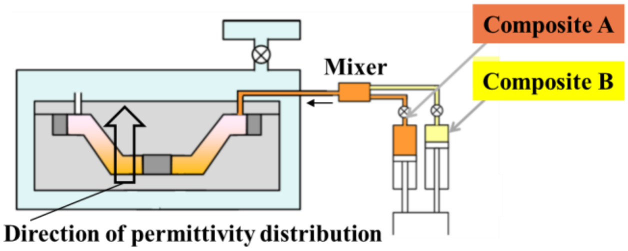

Figure 2. Fabrication concept of cone-type spacer with ε-FGM using the flexible mixture casting method.

The fabrication concept of ε-FGM using the FMC method for a practical cone-type spacer in Figure 2 is as follows:

(1) Filler particles with high permittivity are filled in epoxy resin to prepare the composite A in a tank.

(2) Filler particles with low permittivity are filled in epoxy resin to prepare the composite B in another tank.

(3) Both composites A and B are mixed, continuously and flexibly controlling the mixing ratio using the corresponding valves.

(4) The mixed composites are introduced into a casting mold and accumulated in layers with the controlled mixing ratio, i.e. permittivity distribution in the longitudinal direction, and then cured.

The longitudinal permittivity distribution with the FMC method can also exhibit radial permittivity distribution in the cone-type spacer, which results in electric field grading as principally verified by the centrifugal method. The size distribution of each filler particle is expected to be similar in order to enhance the mechanical and/or thermal properties. The viscosity of both composites A and B can also be controlled via the loading ratio of the filler particles and diluent as well as the temperature of the composites.

2.3 PERMITTIVITY CONTROL USING FMC METHOD

For fabricating ε-FGM using the FMC method, high and low permittivity composites should be prepared. In this section, we verify the controllability in permittivity of composite with different filler particles in epoxy resin. We used $SrTiO_3$ with a relative permittivity (ε_r) of 332 and mean diameter of 9.98 μm, and SiO_2 with ε_r = 3.7 and mean diameter of 8.26 μm, as shown in Table 1. The particle diameter distribution of each filler particle is quite similar, as shown in Figure 3. Both filler particles were filled, stirred and mixed in epoxy resin (Bisphenol-A) using a planetary mixing machine for different loading ratios while keeping their total volume at 40 vol% (vs. total). Then the $SrTiO_3/SiO_2$ composite was put into a post-type mold (diameter: 15 mm, height: 20 mm) and cured in an oven (60 °C for 6 hours and 100 °C for 10 hours). The cured bulk sample was cut into slices (thickness: 1mm), and its capacitance then measured at 1 kHz and converted into permittivity.

Table 1. Specifications of filler particles.

Filler material	$SrTiO_3$	SiO_2
Relative permittivity	332	3.7
Mean diameter [μm]	9.98	8.26
Closest packing fraction [vol%]	40	60

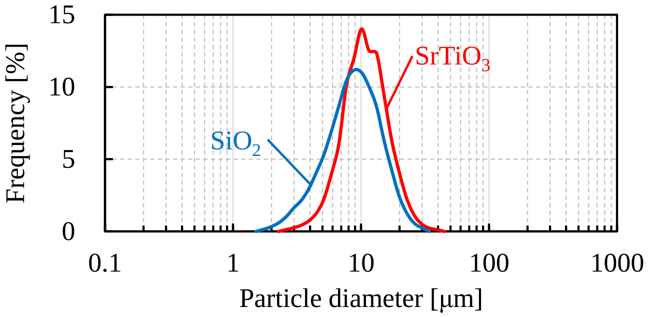

Figure 3. Particle diameter distributions.

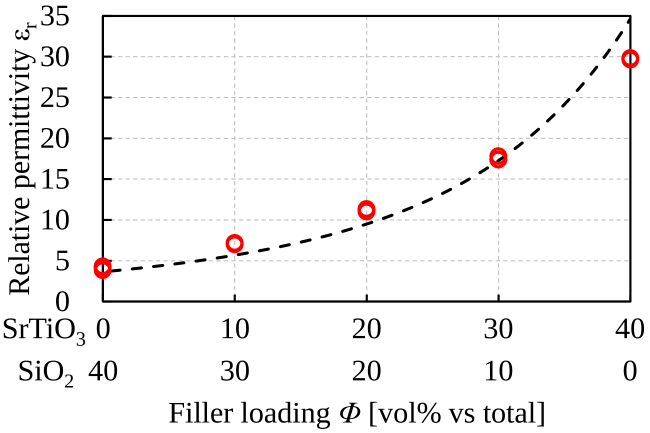

Figure 4. Relative permittivity as a function of filler loading. (circle: measured value, dotted line: calculated value based on modified Bruggeman curve)

Figure 4 shows the relative permittivity of the $SrTiO_3/SiO_2$ composite as a function of their loading ratio. The relative permittivity increased from $\varepsilon_r = 4$ to $\varepsilon_r = 30$ with the increase in the loading ratio of $SrTiO_3$. The broken line in Figure 4 is the modified Bruggeman curve [8,9] of the composite filled with only $SrTiO_3$, which is consistent with the measured values. This result confirms that the relative permittivity of the $SrTiO_3/SiO_2$ composite is determined by the loading ratio of $SrTiO_3$, because the relative permittivity of SiO_2 and epoxy resin is similar. Such a high permittivity ratio and its controllability in Figure 4 using the FMC method can enable the effective electric field grading of ε-FGM.

3 ELECTRIC FIELD RELAXATION BY ε-FGM WITH FLEXIBLE MIXTURE CASTING METHOD

3.1 SIMULATION MODEL

To fundamentally evaluate the electric field relaxation effect of ε-FGM using the FMC method, electric field analysis was carried out for a simplified model of GIS spacer as shown in Figure 5a. The simulation model consists of the inner (HV) and outer (GND) electrodes with coaxial cylindrical configuration, the cone-type spacer and SF_6 gas, and with triple junctions (TJ) on the concave and convex surfaces of the spacer, respectively, i.e. HV-TJ and GND-TJ. The electric field analysis was carried out with the smallest mesh size of about 10 μm around TJs.

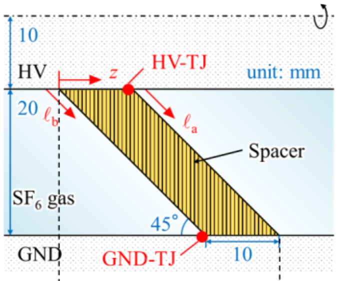

(a) Spacer model

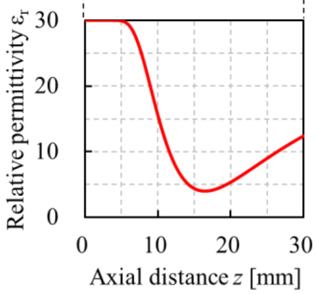

(b) Relative permittivity distribution

Figure 5. Simulation model and relative permittivity distribution of ε-FGM.

Based on our recent works on the permittivity distribution of ε-FGM [10,11], the higher permittivity around HV-TJ and GND-TJ and lower permittivity in between will contribute to electric field grading of cone-type spacers. Then, as an example of such distribution, a relative permittivity distribution in Figure 5b was applied to the spacer with ε-FGM using the FMC method, i.e. a longitudinal permittivity distribution (ε_r = 30 ~ 4 ~ 12) as a function of axial distance (z [mm]) expressed by the following equation:

$$\varepsilon_r(z) = 30 - \frac{530}{z}\exp\left[-\frac{(\ln z - 3.3)^2}{0.082z}\right] \qquad (1)$$

The radial permittivity distribution at a certain position on the z coordinate is assumed to be uniform. For the comparison with ε-FGM, a “uniform case” with a constant relative permittivity ($\varepsilon_r = 4$) for both longitudinal and radial distribution was also applied to the spacer.

3.2 ELECTRIC FIELD RELAXATION

Figure 6 schematically illustrates the electric field distribution around the spacer for different permittivity distributions of (a) uniform case and (b) ε-FGM in Figure 5b. It is easy to find that the localized concentration of electric field strength in the vicinity of HV-TJ in Figure 6a is greatly relaxed in Figure 6b.

Figure 7 shows the electric field strength along the spacer as a function of (a) distance λ_a on the concave surface with HV-TJ and (b) distance λ_b on the convex surface with GND-TJ, from the inner electrode in Figure 5a. The vertical axis shows the ratio E/E_0, i.e. electric field strength normalized via the maximum electric field strength E_0 in the vicinity of HV-TJ in the uniform case. Figures 7a and 7b represent a reduction of E/E_0 in the ε-FGM case to 0.36, i.e. reduced by 64%, improving the uniformity of the electric field distribution compared with that in the uniform case. It should be noted that the maximum electric field strength in the ε-FGM case does not appear in the vicinity of HV-TJ, but in the middle of the convex surface with GND-TJ. This is because the permittivity distribution of ε-FGM in Figure 5b contributed to the increased potential burden in the middle of the convex surface with the lower permittivity.

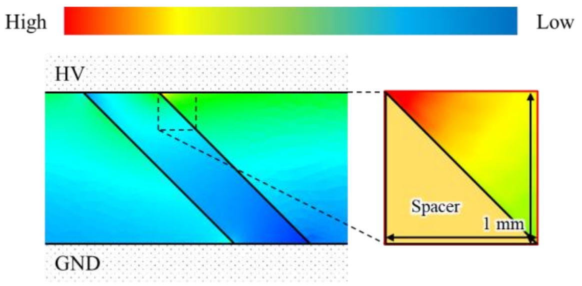

(a) Uniform

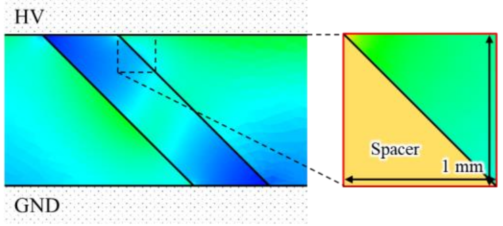

(b) ε-FGM

Figure 6. Electric field distribution around the spacer.

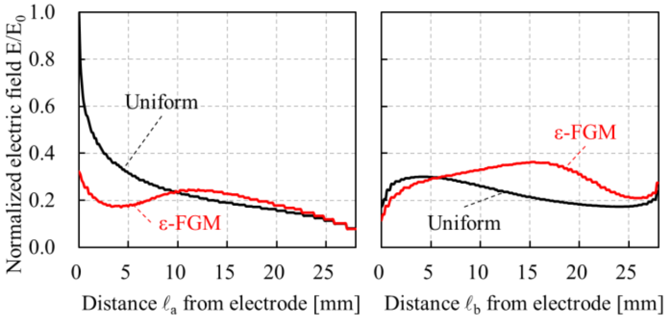

(a) Concave surface with HV-TJ (b) Convex surface with GND-TJ

Figure 7. Electric field strength along the spacer surface.

A similar but other example of ε-FGM with a parabolic permittivity distribution has been discussed for the same spacer configuration in Figure 5a, where $E/E_0 = 0.81$ was obtained [11]. Thus, the electric field relaxation effect depends on the permittivity distribution of ε-FGM in the fixed spacer configuration. The electric field relaxation effect of ε-FGM also depends on the spacer configuration, e.g. shape control of the spacer without TJ, and embedded electrodes, which have different values of E_0. Even in such cases, an appropriate or optimized permittivity distribution of ε-FGM suitable for the spacer configuration and other aspects is expected to be obtained from the given or requested electric field distribution as an inverse problem on ε-FGM using the FMC method.

4 DISCHARGE INCEPTION VOLTAGE IMPROVEMENT BY ε-FGM WITH FLEXIBLE MIXTURE CASTING METHOD

4.1 VOLUME-TIME THEORY

Electric field grading using ε-FGM should be reflected in improved breakdown voltage, leading to smaller-size GIS spacers. Since the breakdown in t SF_6 gas occurs immediately after discharge (streamer) inception under a positive lightning impulse voltage, the breakdown voltage can be evaluated as the discharge inception voltage [12]. In this section, following the electric field analysis in the previous section, the discharge inception voltage in SF_6 gas in the GIS spacer in Figure 5a is theoretically estimated using the volume-time theory. The improvement effect of the discharge inception voltage by ε-FGM using the FMC method is discussed.

The volume-time theory is based on the integration of generation probability of initial electrons and their growth with the electron avalanche in SF_6 gas under a positive lightning impulse voltage. The generation probability P of initial electrons is attributed to desorption from SF_6^- ions in the stressed volume in SF_6 gas and reattachment of generated electrons to SF_6 molecules, as expressed by the following equation [13,14]:

$$P = 1 - \exp\left[\int_t \int_{V_{cr}} \frac{dn_e}{dt}\left(1 - \frac{\eta}{\alpha}\right) dV dt\right] \tag{2}$$

where dn_e/dt is the number of electrons desorbed from SF_6^- ions per unit time and unit volume, which is calculated by the product of SF_6^- ion density and desorption rate coefficient [13]. α is the impact ionization coefficient, and η is the electron attachment coefficient. V_{cr} is the critical volume in SF_6 gas that satisfies $\alpha > \eta$ and Schumann's formula expressed by the following equation:

$$\int_{x_{cr}} (\alpha - \eta) dx = K \tag{3}$$

where $(\alpha - \eta)$ is the effective ionization coefficient, K is a constant, and x_{cr} is the path along the electric line of force. The value of K depends on the gas, and K = 18 for SF_6 gas [15]. For the desorption process, only electron collision desorption is considered. Thus, when an initial electron happens to generate in V_{cr} at a certain time, the electron can grow into an electron avalanche and discharge inception.

According to the above process and equations based on the volume-time theory, the probability of discharge inception is calculated for each applied voltage. The voltage with a probability of 50% is defined as the theoretical discharge inception voltage, $TDIV_{50}$, in SF_6 gas.

4.2 DISCHARGE INCEPTION VOLTAGE IMPROVEMENT

Figure 8 shows $TDIV_{50}$ in SF_6 gas taking into account the entire volume in the simplified GIS spacer model with ε-FGM in Figure 5 as a function of SF_6 gas pressure together with that in the uniform case for comparison. $TDIV_{50}$ with ε-FGM is higher than that in the uniform case at each SF_6 gas pressure, and their difference increases with the increase in SF_6 gas pressure. $TDIV_{50}$ at 0.4 MPa is 70% higher than that in the uniform case. This is the improvement effect of the discharge inception voltage by ε-FGM using the FMC method, which corresponds to the electric field relaxation of 64% in the previous section.

The improvement effect of the discharge inception voltage by ε-FGM in Figure 8 is discussed in terms of the discharge inception point derived from the critical volume V_{cr}. The discharge inception point in the uniform case is always located in the vicinity of HV-TJ on the concave surface in Figure 5. On the other hand, in the case of ε-FGM, Figure 9 schematically indicates the possible discharge inception point at $TDIV_{50}$ for different SF_6 gas pressures. The discharge inception point in the case of ε-FGM can be located not only in the vicinity of HV-TJ, but also in the middle of the convex surface, which is consistent with the higher electric field strength in the middle of the convex surface in Figure 7b..

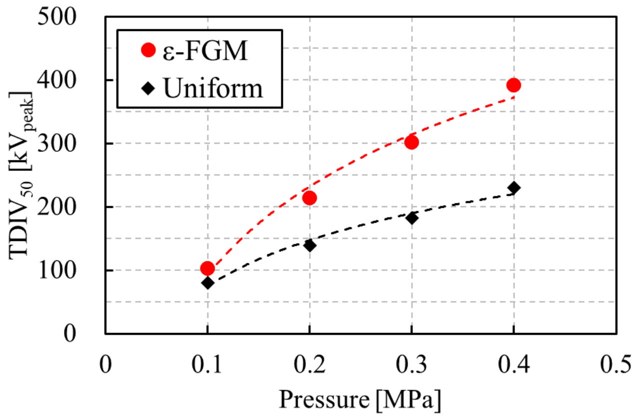

Figure 8. $TDIV_{50}$ in SF_6 gas in the spacer as a function of SF_6 gas pressure.

These results indicate that the improvement effect of the discharge inception voltage by ε-FGM can be attributed to the electric field distribution controlled by ε-FGM, the SF_6 gas pressure and the resultant discharge inception point, i.e. the discharge path length in SF_6 gas satisfying the Schumann's formula. As with the electric field relaxation effect of ε-FGM in the previous section, the discharge inception voltage improvement effect of ε-FGM also depends on the spacer configuration. An appropriate or optimized permittivity distribution of ε-FGM suitable for the spacer configuration is expected to be obtained from the given or requested discharge inception voltage as an inverse problem on ε-FGM using the FMC method.

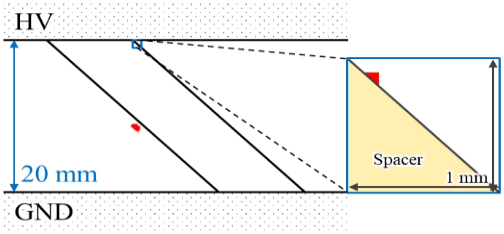

(a) 0.1MPa

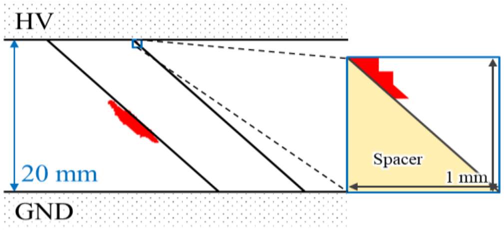

(b) 0.2 MPa

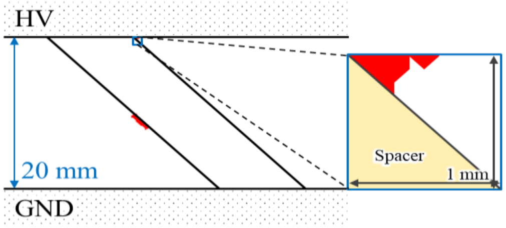

(c) 0.3 MPa

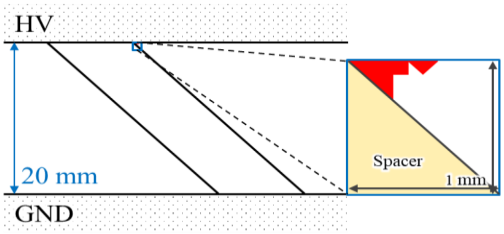

(d) 0.4 MPa

Figure 9. Possible discharge inception points at $TDIV_{50}$ for different SF_6 gas pressures.

5 CONCLUSION

In this paper, we proposed the flexible mixture casting (FMC) method as a novel and practical technique to fabricate permittivity graded materials (ε-FGM). Toward the practical application of ε-FGM, we evaluated the electric field relaxation effect in SF_6 gas in a simplified GIS spacer model with ε-FGM using the FMC method. The discharge inception voltage was also estimated by using the volume-time theory. The main results are summarized as follows:

(1) The relative permittivity of $\varepsilon_r = 4 \sim 30$ was obtained by

the mixture of $SrTiO_3$ and SiO_2 in epoxy resin as a function of the mixing ratio while keeping their total volume at 40 vol%.

(2) When ε-FGM using the FMC method is applied to the simplified spacer model, the maximum electric field strength in SF_6 gas on the spacer surface can be reduced by 64%, compared with that in the case of constant and uniform permittivity.

(3) The discharge inception voltage of the simplified spacer model with ε-FGM can be improved by 70% in SF_6 gas at 0.4 MPa, owing to effective electric field grading by ε-FGM using the FMC method.

The values for the electric field relaxation effect and discharge inception voltage improvement effect of ε-FGM described in this paper depend on the spacer configuration and other aspects, as was described respectively in sections 3.2 and 4.2. Even in such cases, an appropriate or optimized permittivity distribution of ε-FGM suitable for the spacer configuration and other aspects is expected to be obtained as an inverse problem on ε-FGM using the FMC method toward practical application to GIS spacers.

ACKNOWLEDGMENT

This paper is based on results obtained from a project commissioned by the New Energy and Industrial Technology Development Organization (NEDO).

REFERENCES

[1] L. Donzel, F. Greuter and T. Christen: “Nonlinear Resistive Electric Field Grading Part2: Materials and Applications”, IEEE Electr. Insul. Mag., vol. 27, pp. 18-29, 2011.

[2] M. Hering, K. Juhre, M. Secklehner and V. Hinrichsen: “Requirements on Solid Insulating Materials and Gas-Solid Interfaces in Compact HVDC Gas-Insulated Systems”, in *Proceedings of the International Symposium on High Voltage Engineering*, 2017.

[3] G. Eriksson: “High-Field Saturation of Nonlinear Field Grading Materials Used in AC Applications”, in *Annual Report of the Conference on Electrical Insulation and Dielectric Phenomena*, 2017, pp. 1-4.

[4] K. Kato, K. Kimura, S. Sakuma and H. Okubo: “Functionally Gradient Material (FGM) for GIS Spacer Insulation”, in *Proceedings of the International Symposium on High Voltage Engineering*, 2001, pp. 401-404.

[5] M. Kurimoto, K. Kato, M. Hanai, Y. Hoshina, M. Takei and H. Okubo: “Application of Functionally Graded Material for Reducing Electric Field on Electrode and Spacer Interface”, IEEE Trans. Dielectr. Electr. Insul., vol.17, pp. 256-263, 2010.

[6] N. Hayakawa, J. Ishiguro, H. Kojima, K. Kato and H. Okubo: “Fabrication and Simulation of Permittivity Graded Materials for Electric Field Grading of Gas Insulated Power Apparatus”, IEEE Trans. Dielectr. Electr. Insul., vol.23, pp. 547-554, 2016.

[7] A. Kuechler: “*High Voltage Engineering –Fundamentals-Technology-Applications*”, pp.86-89, Springer, 2017.

[8] D. A. G. Bruggeman: “Berechnung verschiedener physikalischer Konstanten von heterogenen Substanzen I. Dielektrizitätskonstanten und Leitfähiegkeiten der Mischkörper aus isotropen Substanzen”, Annalen der Physik, vol.416, pp. 636-664, 1935. (in German)

[9] B. Ploss, B. Ploss, F. G. Shin, H. L. W. Chan and C. L. Choy: “Pyroelectric Activity of Ferroelectric PT/PVDF-TREE”, IEEE Trans. Dielectr. Electr. Insul., vol.7, pp. 517-522, 2000.

[10] N. Hayakawa, Y. Miyaji, H. Kojima and K. Kato: “Electric Field Reduction by Functionally Graded Materials (FGM) with Permittivity and Conductivity Distribution”, in *Annual Report on the Conference on Electrical Insulation and Dielectric Phenomena*, 2016., 6A-27.

[11] N. Hayakawa, Y. Miyaji, K. Ochiai, H. Kojima and K. Kato: “A Novel Fabrication Technique of Permittivity Graded Materials by Flexible Mixture Casting Method for GIS Spacers”, in *Proceedings of the International Symposium on High Voltage Engineering*, 2017.

[12] K. Kato, M. Kurimoto, H. Shumiya, H. Adachi, S. Sakuma, H. Okubo: “Application of Functionally Graded Material for Solid Insulator in Gaseous Insulation system”, IEEE Trans. Dielectr. Electr. Insul., vol.13, pp. 362-371, 2006.

[13] X. Xu, S. Jayaram and S. A. Boggs: “Prediction of Breakdown in SF_6 under Impulse Conditions”, IEEE Trans. Dielectr. Electr. Insul., vol.3, , pp. 836-842, 1996.

[14] H. Okubo, H. Shumiya, M. Ito and K. Kato: “Insulation Performance of Permittivity Graded FGM (Functionally Graded Materials) in SF_6 Gas under Lightning Impulse Conditions”, in *Proceedings of the IEEE International Symposium on Electrical Insulation*, 2006, pp.332-335.

[15] H. Hanai, T. Teranishi, H. Okubo and S. Yanabu: “Insulating Characteristics of SF_6 Small Gas Gaps against Lightning Impulse Voltages”, J. IEE Jap., vol. 109-A, pp. 255-262 (1989) (in Japanese)

Naoki Hayakawa (M’90) was born on September 9, 1962. He received a Ph.D. degree in 1991 in electrical engineering from Nagoya University. He has been at Nagoya University since 1990, where he is presently a Professor in the Department of Electrical Engineering. From 2001 to 2002, he was a guest scientist at the Forschungszentrum Karsruhe, Germany. Prof. Hayakawa is a member of IEE of Japan and CIGRE.

Yoshitaka Miyaji was born on January 31, 1993. He received an M.S. degree in electrical engineering in 2017 from Nagoya University. Mr. Miyaji is a member of IEE of Japan.

Hiroki Kojima (M’11) was born on December 7, 1975. He received a Ph.D. degree in 2004 in energy engineering and science from Nagoya University. He has been at Nagoya University since 2004, where he is presently an Associate Professor in the Department of Electrical Engineering. Dr. Kojima is a member of IEE of Japan.

Katsumi Kato was born on May 20, 1969. He received a Ph.D. degree in 1997 in electrical engineering from Nagoya University. From 1997, he was on the faculty of Nagoya University. Currently he is an Associate Professor at the National Institute of Technology, Niihama College in the Department of Electrical Engineering and Information Science. Dr. Kato is a member of IEE of Japan.